Available online at www.sciencedirect.com
SCIENCE DIRECT®
Coordination Chemistry Reviews 249 (2005) 1582–1595
COORDINATION CHEMISTRY REVIEWS
www.elsevier.com/locate/ccr

Review

Chemistry relating to the nickel enzymes CODH and ACS

David J. Evans*

Department of Biological Chemistry, John Innes Centre, Norwich Research Park, Norwich NR4 7UH, UK

Received 30 July 2004; accepted 18 September 2004
Available online 13 November 2004

Contents

Abstract

The nickel enzymes CODH and ACS (carbon monoxide dehydrogenase and acetyl-CoA synthase), as found in for example *Moorella thermoacetica* (formerly *Clostridium thermoaceticum*), play an important role in carbon cycling: the enzymes convert carbon dioxide through to cell carbon. CODH and ACS are neither structurally nor functionally related to NiFe-hydrogenase, other than that all three enzymes contain assemblies of iron, nickel and sulfur at their active sites. However, the coordination chemistry of synthetic compounds that show structural or functional analogy to the enzyme active sites has been developed in parallel. Herein will be described mono-, di- and multi-nuclear metallic complexes of relevance to the metallocentres of CODH and ACS.

Keywords: Carbon monoxide dehydrogenase; Acetyl-CoA synthase; Nickel enzymes

* Tel.: +44 1 603 450706; fax: +44 1 603 450018.
E-mail address: dave.evans@bbsrc.ac.uk.

0010-8545/$ – see front matter © 2004 Elsevier B.V. All rights reserved.
doi:10.1016/j.ccr.2004.09.012

1. Introduction

The water-gas shift reaction (WGSR) and the Reppe process (RP) are extremely important to industry. The WGSR utilises the reducing power of CO to generate CO_2 and hydrogen from water at high temperature, Eq. (1), with expensive catalysts based on chromium and ruthenium. The hydrogen produced is used, for example, as the reductant in the Haber-Bosch process for the synthesis of ammonia from dinitrogen.

$$CO + H_2O \rightarrow CO_2 + H_2 \quad (1)$$

The RP synthesizes acetic acid from methanol and CO using a rhodium-based (Monsanto) or iridium-based (BP Chemicals) catalyst at 180–220 °C and 30–40 bar. This process generates 10^6 tons of acetic acid annually worldwide. In contrast, the enzymes nickel CO-dehydrogenase (CODH) and acetyl-CoA synthase (ACS) can perform the equivalent conversions, under physiological conditions, with active sites consisting of the much cheaper metals iron and nickel [1,2]. The CODH reaction, Eq. (2), is formally equivalent to the WGSR except the former produces two protons and two electrons and the latter produces hydrogen.

$$CO + H_2O \leftrightarrow CO_2 + 2H^+ + 2e^- \quad (2)$$

The ACS reaction (the synthesis of acetyl-CoA by the non-redox condensation of a methyl group, a carbonyl group and an organic thiol) parallels the RP, both apparently involving metal-carbonyl, methyl-metal and acyl-metal intermediates. In addition, through the coupled reactions of CODH/ACS, CO_2 and highly toxic CO, an inhibitor of essential metalloenzymes, are not only removed from the environment but are used as a source of cell carbon and electrons. These conversions are of current relevance to the need to reduce carbon oxide emissions from industry and their levels in the environment and to develop alternative routes to chemical feedstocks. The design of bioinspired synthetic assemblies may provide cheaper catalysts for use in these important industrial and environmental processes.

2. Enzyme structure and function

2.1. Distribution

Unifunctional CODH (i.e. the enzyme has no ACS function) is found in anaerobic bacteria such as *Rhododspirillum rubrum* and *Carboxydothermus hydrogenoformans* that utilise CO for growth. The CODH enzymes are coupled to a membrane bound CO-induced hydrogenase that together can catalyse oxidation of CO to CO_2 with formation of hydrogen; this allows the organisms to grow with CO as the only energy source [3,4]. Bifunctional CODH/ACS (i.e. the enzyme has both CODH and ACS function) are found in acetogenic bacteria, e.g. *Moorella thermoacetica* (formerly *Clostridium thermoaceticum*), where they catalyse the synthesis of acetyl-CoA, allowing autotrophic growth on CO_2 or CO by the Wood–Ljungdahl carbon fixation pathway, and in methanogenic archaea, e.g. *Methanosarcina thermophila* and *M. barkeri*, where the disassembly of acetyl-CoA is catalysed facilitating the utilisation of acetate in metabolism and generating methane (in this case the multienzyme complex is better described as an acetyl-CoA decarbonylase/synthase, ACDS) [5]. The organisms that contain CODH and ACS are some of the most evolutionary primitive; the reactions that these enzymes catalyse may have allowed the earliest forms of life to prosper, as has been postulated by Wächtershäuser [6].

2.2. Carbon monoxide dehydrogenase (CODH)

2.2.1. Structure

The unifunctional CODH from *C. hydrogenoformans* is a homodimeric protein of approximately 130 kDa. The dimer contains five metal-sulfur clusters: two B, two C and D. The crystal structure (1.6 Å resolution) of the reduced CODH protein shows the active centre, C-cluster, to be a unique asymmetric $\{NiFe_4S_5\}$ assembly (Fig. 1a) [7]. The nickel is four-coordinate, square planar and one of the iron atoms is extraneous to the cuboidal-like core, linked to nickel through a μ_2-bridging-sulfide.

The crystal structure (2.8 Å resolution) of the non-reduced, CO preincubated CODH C-cluster from *R. rubrum*

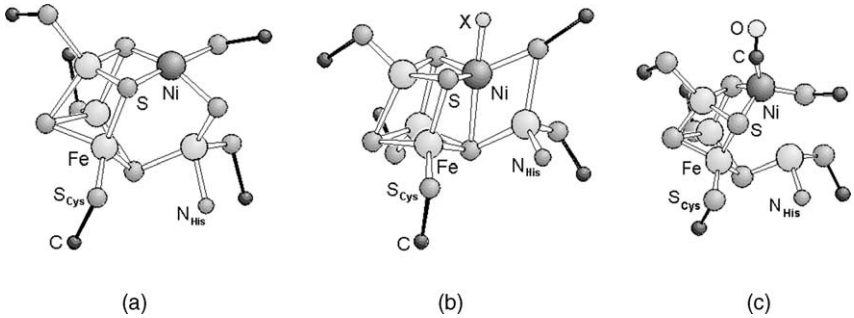

Fig. 1. The structures of CODH C-cluster: (a) reduced form in *C. hydrogenoformans* [7]; (b) non-reduced, CO preincubated form in *R. rubrum* [8]; (c) from CODH/ACS in *M. thermoacetica* [9].

shows nickel to be at the corner of a cuboidal cluster, five-coordinate, with a ligand (X) assigned as bound CO (Fig. 1b) [8]. The iron atom is linked to nickel not through a bridging-sulfide but by a bridging cysteinyl-sulfur. A third variant of C-cluster has been reported for CODH in the bifunctional CODH/ACS from *M. thermoacetica* with (at 1.9 Å resolution, Fig. 1c) [9] and without (at 2.2 Å resolution) [10] a CO ligand modelled in the apical coordination site of the nickel. Here there is apparently no direct link between the nickel atom and the extraneous iron. In addition, the four Ni–Fe distances vary from structure to structure. For example, in the *C. hydrogenoformans* structure the Ni–Fe distances range over almost 1 Å (2.8–3.7 Å), but in the *R. rubrum* structure the spread of the distances is considerably less (2.6–2.8 Å). The discrepancy between the different structures may be attributed to uncertainties of fitting lower-resolution data, different protein crystallisation conditions, differences in the protein structures themselves or different chemical states of the same cluster [8,11,12]. It has been demonstrated that redox-dependent structural rearrangement can occur on treatment with CO [13]. Others have proposed that CODH activity is dependent on the presence of the μ_2-bridging-sulfide in C-cluster and that those clusters lacking the μ_2-bridging-sulfide are inactive and are formed by CO induced decomposition [14]. In contradiction to this, it has been shown that addition of sulfide to CODH lacking the μ_2-bridging-sulfide inhibits CO oxidation [15].

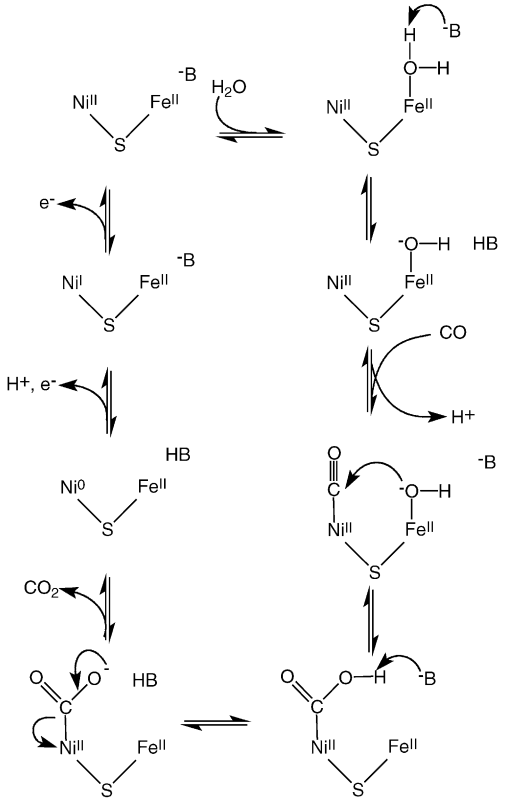

Scheme 1.

2.2.2. Mechanism

A proposed catalytic mechanism of CODH action is shown in Scheme 1 [11]. Water is bound to the extraneous iron atom of the C-cluster, a nucleophilic hydroxide is generated that then attacks CO bound at the adjacent nickel. The resultant carboxylic acid group bound at nickel is deprotonated and, on delivery of two electrons to the active site, CO_2 is lost. However, details of the mechanism remain contentious [15] and further experimentation is required.

2.3. Acetyl-CoA synthase (ACS)

2.3.1. Structure

Protein crystallography of *M. thermoacetica* CODH/ACS bifunctional enzyme has shown it to be a 310 kDa $\alpha_2\beta_2$ heterotetramer [9,10]. The β-domains have structures similar to those of the unifunctional CODH described above and contain the B-, C- and D-clusters. On each end of the complex are the α-domains containing A-cluster that is responsible for

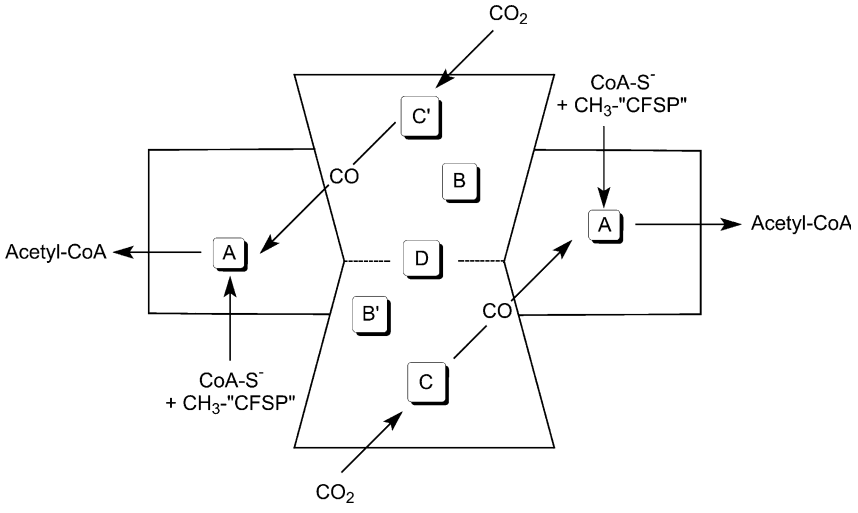

Fig. 2. Schematic representation of CODH/ACS protein structure showing the various clusters and reactions catalysed. “CFSP”: corrinoid-iron-sulfur-protein.

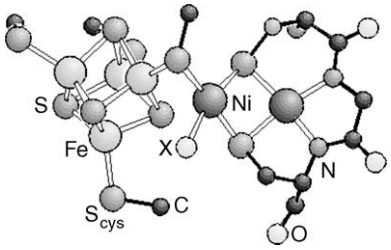

Fig. 3. Crystal structure of the A-cluster of ACS [9].

ACS activity (Fig. 2). Hydrophobic channels through which gases can pass from one active site to the other connect A- and C-clusters. A-cluster is comprised of an Fe_4S_4-cluster bridged through cysteinyl-thiolate sulfur to a proximal metal that is then linked to a distal nickel(II) atom in an N_2S_2 coordination environment (Fig. 3). The N_2S_2 coordination is provided for by a deprotonated Cys-Gly-Cys sequence of the protein. The proximal metal was first determined to be tetrahedral copper(I) [10]. A later study identified the proximal metal as tetrahedral zinc(II) in a closed protein conformation and as square planar nickel(II) in an open conformation of the protein [9]. Functional monomeric ACS from *C. hydrogenoformans* also contains an $\{Fe_4S_4\}$–Ni–Ni assembly [16] and X-ray absorption spectroscopy (XAS) has established the presence of a similar unit in A-cluster of ACDS complex of *M. thermophila* [17]. The current consensus is that the enzymatically active A-cluster possesses a proximal nickel atom (Fig. 3), for which the fourth ligand remains unidentified, but that this atom is labile and under certain conditions it may be replaced by copper or zinc to give inactive enzyme [18–21].

2.3.2. Mechanism

Scheme 2 shows a possible enzymatic mechanism for ACS [9,22,23]. The proximal nickel atom, which sits below a gas channel, first binds CO. A methyl group is then transferred from methylated-corrinoid-iron-sulfur protein to the same nickel while the nickel gains two electrons. The axially bound CO then inserts into the nickel-methyl bond to generate a nickel-acetyl which in turn is attacked by deprotonated CoA, giving acetyl-CoA product. The Fe_4S_4-cluster and the distal nickel atom are not thought to play a role in the redox events of the catalytic cycle.

An alternative mechanism is shown in Scheme 3 [24]. In this paramagnetic cycle CO binds to a nickel(I) site which then performs nucleophilic attack on the methylated-corrinoid-iron-sulfur protein to generate a nickel(III)-methyl species which is rapidly reduced to nickel(II)-methyl. This is followed by a CO insertion (or methyl migration) to give nickel-acetyl, which is deacetylated by deprotonated CoA to give acetyl-CoA. The last step can occur either by thiol nucleophilic attack on the nickel-acetyl or by the deprotonated CoA first binding to the A-cluster; the thioester is then formed by reductive elimination.

In both proposed mechanisms the CO is shown to bind first although this has not been unequivocally demonstrated by experiment. As has been discussed recently [25], the first mechanism requires the ordered binding of CO and the methyl group and is precedented by the oxidative addition of CH_3X to nickel(0) whereas the latter mechanism is not balanced with respect to electron count and metal oxidation level.

3. Chemistry relating to CODH

3.1. Structural models before the CODH protein crystal structure

Before the protein crystal structure of CODH was reported the C-cluster was initially considered to be, based on various spectroscopic techniques (EPR, ENDOR, Raman, Mössbauer) and XAS, an Fe_4S_4-cubane cluster linked to nickel(II) through a single bridging atom, probably sulfur.

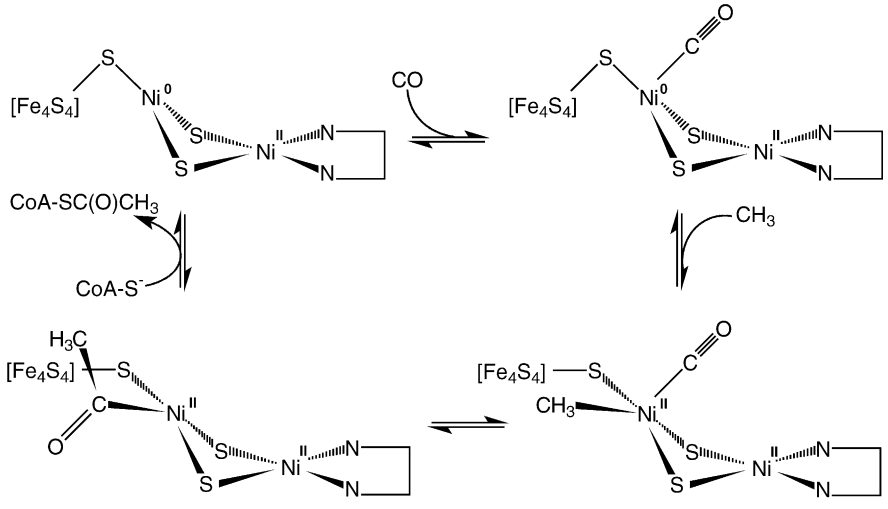

Scheme 2.

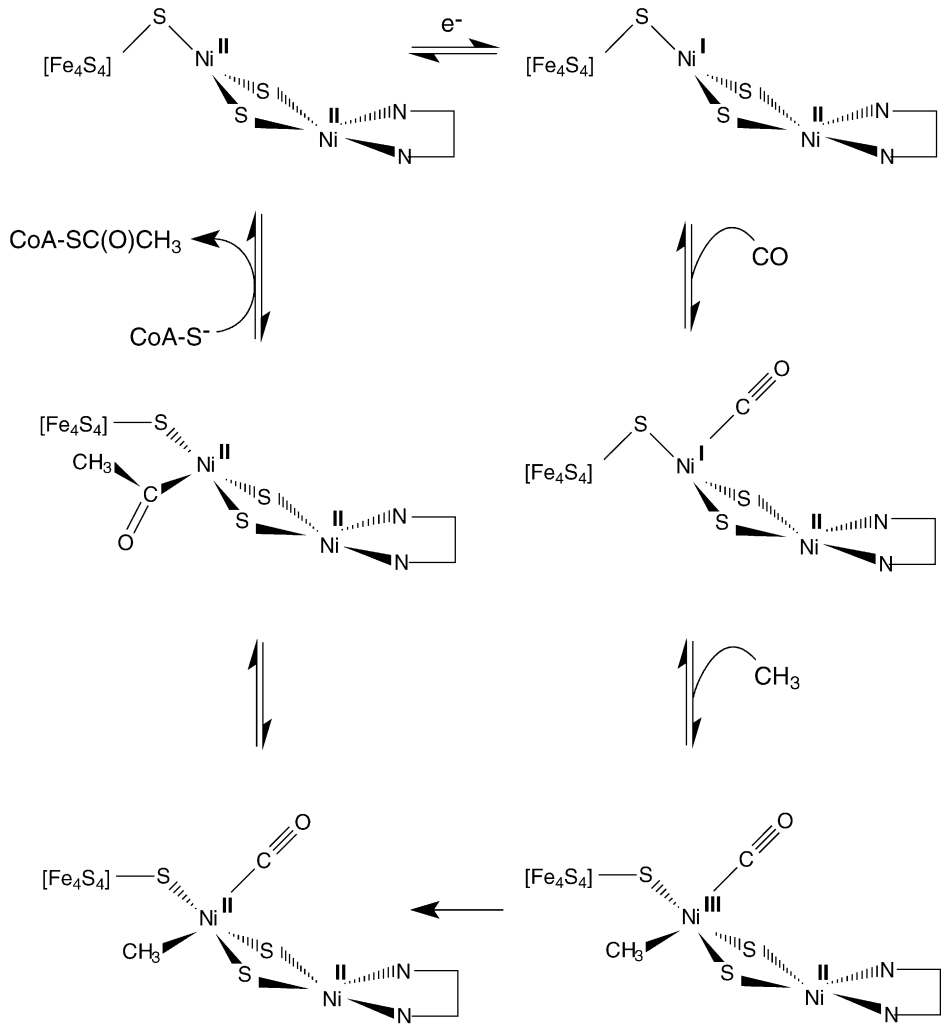

Scheme 3.

The nickel was predicted to be five-coordinate, the coordination sphere being completed by one additional sulfur and three nitrogen or oxygen ligands (Fig. 4a) [1,2]. Attempts to construct such assemblies led Pohl and co-workers to the synthesis of Fe_4S_4-cubanes linked to nickel(II) in an N_2S_2 coordination environment [26]. The assemblies (Fig. 5) have two Ni–N_2S_2 units bound to the cubane core either through two μ-sulfurs in $[\{NiL\}_2Fe_4S_4I_2]$ or one μ-sulfur in $[\{NiL\}_2Fe_4S_4(Stip)_2]$ (L = *N*,*N*′-diethyl-3,7-diazanonane-1,9-dithiolate; tip = 2,4,6-triisopropylbenzene). A preliminary structure of a related compound $[\{NiL\}Fe_4S_4I_3]$ was also reported where one $\{NiL\}$ unit has been linked to an Fe_4S_4-cluster (Fig. 6) [27]. Later, it was proposed that the C-cluster contained a binuclear FeNi-fragment linked, probably, through cysteinyl-sulfur to an Fe_4S_4-cluster [28]. The iron(II) and nickel(II) atoms within the diheterometallic unit were said to be bridged through two cysteinyl-sulfurs and, in addition, that there was a nitrogen from histidine and a molecule of non-substrate CO bound to the iron(II) atom, the other ligands were not identified (Fig. 4b). In our laboratory we utilised the iron(II)-carbonyl chelate, $[Fe(NS_3)(CO)]^-$ where NS_3H_3 is $N(CH_2CH_2SH)_3$ [29], to prepare the structurally characterised trinuclear complex $[Ni\{Fe(NS_3)(CO)\text{-}S,S'\}_2]$ (Fig. 7) which had structural similarities to the proposed C-cluster structure. Common features included (Fig. 4c): N and CO coordinated to iron(II); iron bridged through two μ_2-thiolate sulfurs to nickel; nickel bridged through a further thiolate sulfur to another iron atom. In the C-cluster the nickel was predicted to have square planar geometry but in the model complex the geometry about nickel is almost regular tetrahedral, unusual for nickel(II) in an all thiolate coordination environment [30,31]. However, as we have seen the active site structure was not as predicted.

3.2. Structural models after the CODH protein crystal structure

When the CODH structure was first reported in 2001 the topology of the active centre C-cluster came as a surprise to all. The unique $\{NiFe_4S_5\}$ assembly had no precedent either in biology or chemistry. To approach a rational synthesis to such an assembly there are at least two requirements:

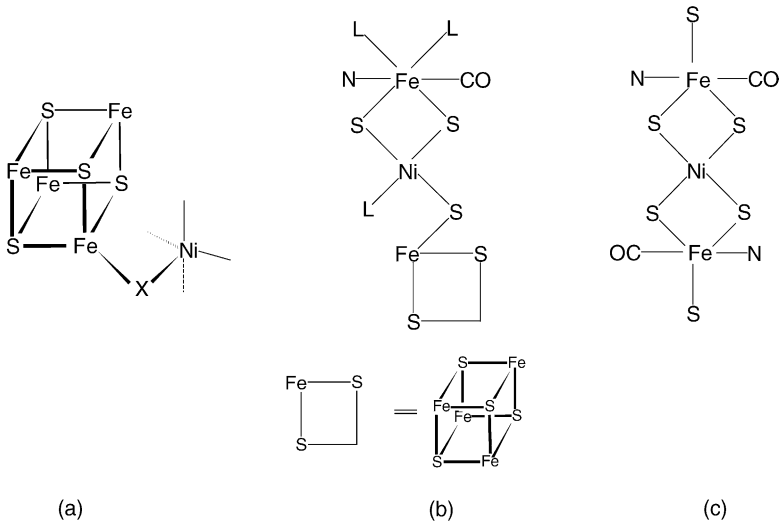

Fig. 4. (a) and (b) proposed structures for CODH C-cluster before the protein structure was determined and (c) the core of [Ni{Fe(NS_3)(CO)-S,S'}$_2$].

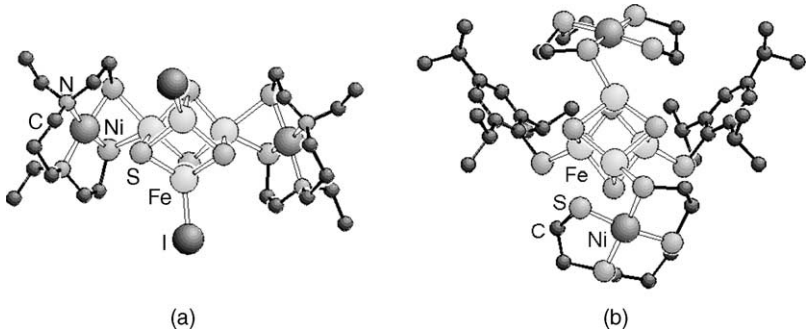

Fig. 5. The crystal structures of [{NiL}$_2$Fe$_4$S$_4$I$_2$] and [{NiL}$_2$Fe$_4$S$_4$(Stip)$_2$] [26].

that there is an *exo*-iron atom linked through sulfide to a {NiFe$_3$S$_4$} fragment and that the nickel(II) atom has square planar geometry. Heterometallic clusters bound by *exo*-iron atoms bridged through thiolate have been described but none involve sulfide bridges. For example, we have synthesised from the iron-bridged dicubane [NEt$_4$]$_3$[Mo$_2$Fe$_7$S$_8$(SEt)$_{12}$], by reaction with π-acid ligands, {MoFe$_3$S$_4$}$^{3+}$ clusters linked to an *exo*-iron. Two of these, [NEt$_4$][MoFe$_3$S$_4$X$_3$(μ-SEt)$_3$Fe(CN^{t}Bu)$_3$] where X is Cl (Fig. 8) or SPh, have been crystallographically characterised. The *exo*-iron centre is in the low-spin iron(II) state and there is little electronic interaction between the cubane and *exo*-iron [32]. A related complex, [NEt$_4$]$_2$[MoFe$_3$S$_4$(SC$_6$H$_{11}$)$_3$(μ-SC$_6$H$_{11}$)$_3$Fe(SC$_6$H$_{11}$)], can be prepared directly from a reaction system containing FeCl$_2$, NaSC$_6$H$_{11}$, [NH$_4$]$_2$[MoS$_4$] and [NEt$_4$][BF$_4$] [33].

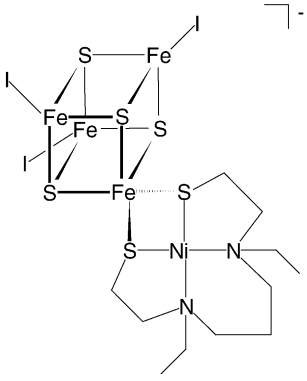

Fig. 6. Schematic representation of [{NiL}Fe$_4$S$_4$I$_3$]$^-$ [27].

Holm and co-workers have developed the closest synthetic analogues of the {NiFe$_3$S$_4$} fragment; mostly before the enzyme structures were reported. Reaction of linear trinuclear iron(III) complex [NEt$_4$]$_3$[Fe$_3$S$_4$(SEt)$_4$] with [Ni(PPh$_3$)$_4$] leads to reductive rearrangement of the

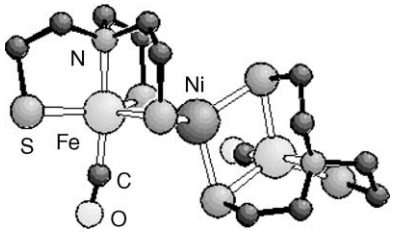

Fig. 7. Crystal structure of the molecule [Ni{Fe(NS_3)(CO)-S,S'}$_2$] [30,31].

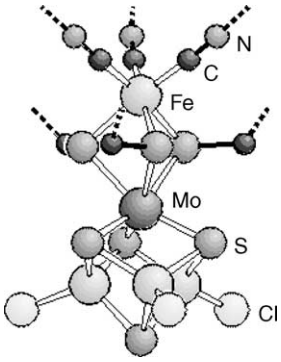

Fig. 8. Crystal structure of the anion $[MoFe_3S_4Cl_3(\mu\text{-}SEt)_3Fe(CN^tBu)_3]^-$ showing an *exo*-iron atom bound to the $\{MoFe_3S_4\}^{3+}$ core, Et and ^{t}Bu groups omitted for clarity [32].

starting complex to a cuboidal fragment and capture of the nickel atom to give $[NEt_4]_2[NiFe_3S_4(PPh_3)(SEt)_3]$ (Fig. 9a) and, in a separate work up, $[NEt_4]_3[NiFe_3S_4(SEt)_4]$ [34]. Similarly, the cluster $[NEt_4]_2[NiFe_3S_4(PPh_3)(Smes)_3]$, where Smes is mesitylthiolate(1−), could be prepared. However, $[NEt_4]_3[NiFe_3S_4(Smes)_4]$ could only be obtained as a 1:1 mixture with $[NEt_4]_2[Fe_4S_4(Smes)_4]$ from the reaction of the linear complex $[NEt_4]_3[Fe_3S_4(Smes)_4]$ and $[Ni(AsPh_3)_4]$ [35]. An alternative approach taken by Holm is to incorporate nickel into a pre-formed voided-cuboidal $\{Fe_3S_4\}$ cluster by an inner-sphere redox reaction [36]. Reaction of $[NEt_4]_3[Fe_3S_4(L'S_3)]$, where $L'S_3$ is 1,3,5-tris((4,6-dimethyl-3-mercaptophenyl)thio)-2,4,6-tris(*p*-tolylthio)benzene(3−), with $[Ni(PPh_3)_3Cl]$ affords $[NEt_4]_2[(Ph_3P)NiFe_3S_4(L'S_3)]$. In all of these $\{NiFe_3S_4\}^+$ clusters the nickel(II) is tetrahedrally coordinated. However, it should be emphasised that none of these clusters possess the required *exo*-iron atom.

Recently, the coordination geometry about nickel in $[NEt_4]_2[(Ph_3P)NiFe_3S_4(L'S_3)]$ has been modified from tetrahedral to planar diamagnetic nickel(II) [37]. The stereochemical conversion is effected by the binding of 1,2-bis(dimethylphosphino)ethane (dmpe), a ligand that generates a sufficiently strong in-plane ligand field. So, reaction of $[NEt_4]_2[(Ph_3P)NiFe_3S_4(L'S_3)]$ with dmpe gave $[NEt_4]_2[(dmpe)NiFe_3S_4(L'S_3)]$. In the reaction the initial axial triphenylphosphine is lost, one Ni–(μ_3-S) bond is broken, and $[Fe_3(\mu\text{-}S)(\mu_3\text{-}S)_3]^-$ and distorted planar $Ni^{II}(\mu_3\text{-}S)_2P_2$ fragments are generated (Fig. 9b). In the solvated cluster four crystallographically distinct edge-cleaved cubanes are present with different non-bonding Ni···S interactions that range from 2.60 to 2.90 Å. The structure, with its edge-cleaved cubane core and planar nickel(II) site, presents the first step towards a synthetic route to a closer analogue of the CODH C-cluster.

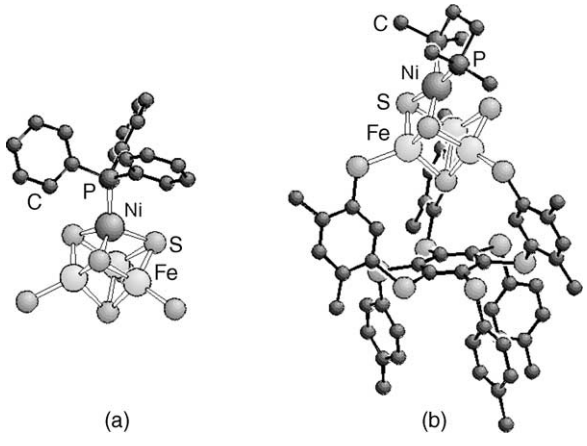

Fig. 9. Crystal structure of the cluster dianions (a) $[NiFe_3S_4(PPh_3)(SEt)_3]^{2-}$, Et groups omitted for clarity [34] and (b) $[(dmpe)NiFe_3S_4(L'S_3)]^{2-}$ [37].

3.3. Towards functional models of CODH

3.3.1. Monometallic systems

Many nickel complexes and their interactions with CO and CO_2 had been described prior to the structure of the C-cluster being defined. These have been previously reviewed [1]. Here the discussion will be restricted to two systems in which nickel is in an environment of sulfur and to a system where a nickel complex catalyses the conversion of CO to CO_2 in aqueous solution.

The potential for square-planar nickel to bind CO has been demonstrated in a complex in which nickel(II) is bound by a thiolato-thioether ligand, [Ni(tpttd)], where H_2tpttd is 2,2,11,11-tetraphenyl-1,5,8,12-tetrathiadodecane (Fig. 10). On electrochemical reduction a fairly stable reduced state is achieved in a reversible process. Under CO the reversibility is lost and the paramagnetic nickel(I)-carbonyl species $[Ni(tpttd)(CO)]^-$, Eq. (3), is generated which exhibits an infra-red υ_{CO} at 1940 cm^{-1}. This nickel(I)-carbonyl was not structurally characterised [38]:

$$[Ni(tpttd)] + e^- \leftrightarrow [Ni(tpttd)]^- + CO \rightarrow [Ni(tpttd)(CO)]^- \quad (3)$$

A rare example of a nickel(II)-carbonyl, with thiolate ligands to nickel, has also been reported and structurally characterised. A nickel complex of the tripodal phosphine trithiolate ligand tris(3-phenyl-2-thiophenyl)phosphine (*PS3*) upon addition of CO and an appropriate counterion yields the diamagnetic complex $[N^nBu_4]_2[Ni(PS3)(CO)]$. The infra-red υ_{CO} is observed at 2029 cm^{-1} and the crystal structure (Fig. 11) shows a distorted trigonal bipyramidal structure with the CO axial and *trans* to phosphorus. Attempts to oxidise the

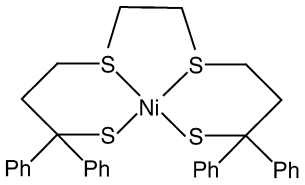

Fig. 10. $[Ni(tpttd)_2]$ a thiolato-thioether ligated nickel(II) complex.

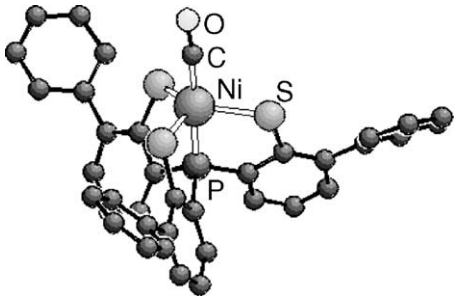

Fig. 11. The crystal structure of the $[Ni(PS3)(CO)]^{2-}$ anion [39].

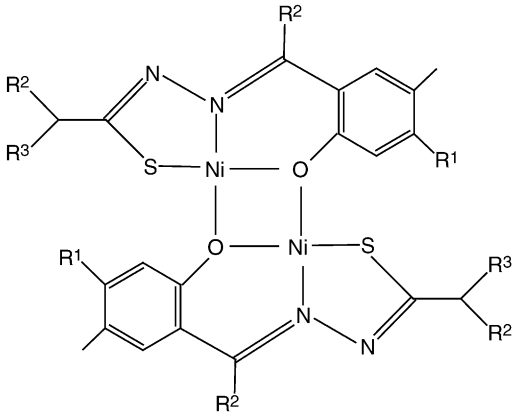

Fig. 12. $[Ni(tmtss)]_2$: (a) $R^1 = R^2 = Me$; $R^3 = H$; (b) $R^1 = H$; $R^2 = R^3 = Me$; (c) $R^1 = R^2 = R^3 = Me$.

nickel(II)-carbonyl to nickel(III) led to loss of CO [39]. Neither of these nickel(I)- nor nickel(II)-carbonyl complexes facilitates conversion of CO to CO_2.

A catalytic system that does oxidise CO to CO_2, at room temperature in aqueous solution (CH_2Cl_2/MeOH/H_2O), with electron transfer to methylviologen utilises nickel(II)iminothiolates, $[Ni(tmtss)]_2$ (Fig. 12, tmtss is substituted 2-hydroxyacetophenone-thiosemicarbazonato) [40]. The proposed mechanism is shown in Scheme 4. Initially, CO binds to the methanol solvated monomeric form of the catalyst; the attached CO is susceptible to nucleophilic attack by water to give Ni–COOH. The

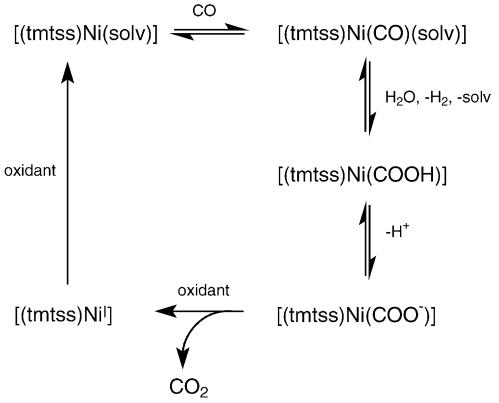

Scheme 4.

Ni–COOH rapidly deprotonates allowing decarboxylation induced by methylviologen oxidation resulting in a nickel(I) complex, a proton and CO_2. Finally, the methylviologen rapidly oxidises the nickel(I) intermediate back to nickel(II). The absence of any hydrogen product can be explained by the absence of a nickel(I)-hydride species that would be required for hydrogen formation by protonation. As in the enzymatic system cyanide inhibits the catalytic system [40]. This catalytic system provides a precedent for the involvement of a Ni(II) centre in the enzymatic oxidation of CO in CODH.

3.3.2. *Dimetallic systems*

The mechanism of action of CODH is now thought to involve adjacent iron and nickel atoms bridged through sulfur (see Section 2.2.2). Dimetallic systems containing nickel and iron have been synthesised in the context of preparing structural/functional analogues for the active site of NiFe-hydrogenase [41]. Early examples include $[\{NiL''\text{-}S\}Fe(CO)_4]$ ($H_2L'' = N,N'$-bis(ethanethiol)-1,5-diazacyclooctane) [42] and $[\{NiL^{\#}\text{-}S,S'\}Fe(NO)_2]$ ($H_2L^{\#} = N,N'$-diethyl-3,7-diazanonane-1,9-dithiol) [43]. We have prepared the iron-dicarbonyl complexes $[\{Fe(NS_3)(CO)_2\text{-}S,S'\}NiCl(diphos)]$, where diphos is dppe, 1,2-bis(diphenylphosphino)ethane [31,44], or dppp, 1,2-bis(diphenylphosphino)propane [45] and the monocarbonyl-iron complex $[\{Fe(NS_3)(CO)\text{-}S,S'\}NiCl(dppe)]$ [30]. In each of these complexes the $\{Fe(NS_3)\}$ unit acts as a chelate ligand linking the iron(II) and nickel(II) through two thiolate sulfurs. Other related dimetallic complexes such as $[\{Ni(SCH_2CH_2CH_2S)(dppe)\text{-}S,S'\}Fe(CO)_3]$ [46] and $[\{Fe(S_3)(CO)(PMe_3)_2\text{-}S,S'\}Ni(S_2)]$ (S_3^{2-} = bis(2-mercaptophenyl)sulfide(2−) and S_2^{2-} = 1,2-benzenedithiolate(2−)), in which the nickel atom is in an all-sulfur coordination environment [47], have also been reported. Some of these dimetallic complexes, although not good structural analogues of the C-cluster, may lead to chemical systems of relevance to the mechanism of CODH but, as yet, they are untested.

4. Chemistry relating to ACS

4.1. *Structural models before the ACS protein crystal structure*

The A-cluster at the active site of ACS was proposed to be, based on spectroscopy and XAS and before the protein crystal structure was published, a bridged assembly $\{Ni\text{–}X\text{–}Fe_4S_4\}$, similar to that proposed for the C-cluster before the CODH crystal structure. The bridging atom was unidentified and the nickel(II) was thought to be distorted square planar, bound by two sulfur ligands and two nitrogen or oxygen ligands. Of some relevance to this proposed active site were the Fe_4S_4-cubanes linked to nickel(II) described above [26,27]. Holm and co-workers took an alternative approach by designing

and synthesising helix-loop-helix 63 residue peptides as scaffolds to stabilise the required complex metal assemblies [48]. The peptides consist of two helices, with about 20 amino acid residues, which are connected by a flexible loop containing the ferredoxin consensus sequence Cys-Ile-Ala-Cys-Gly-Ala-Cys that can bind an Fe_4S_4-cluster. In addition, a fourth cysteine was positioned so as to provide a bridging group between the cluster and nickel(II) and three other binding groups (three histidine or two histidine and one cysteine) were positioned to provide an appropriate binding site for the nickel. Products obtained from reaction of the peptides with $[Fe_4S_4(SCH_2CH_2OH)_4]^{2-}$ followed by, after purification, reaction with a nickel salt exhibited X-ray absorption spectra consistent with incorporation of Fe_4S_4 at the predicted site and supported the existence of distorted square planar nickel either as $[Ni(Cys)(His)_3]$ or $[Ni(Cys)_2(His)_2]$, respectively, bridged through one of the cysteinyl sulfurs to the cluster [49,50]. However, although this work demonstrated the utility of de novo designed peptides to provide scaffolds for stabilisation of complex metal sites, the crystal structure of the active site when published "moved the goalposts", showing the A-cluster to be not as simple as predicted.

4.2. Dimetallic structural models after the ACS protein structure

The crystal structures of ACS showed the active site to be an $\{Fe_4S_4\}$–M–Ni assembly as described above (see Section 2.3.1 and Fig. 3). This unprecedented structure set a new synthetic target for bioinorganic/coordination chemists. Initially, the approach to be taken will put aside the Fe_4S_4 unit and attempts will be made to synthesise structural analogues of the dinuclear sub-site. The first reported enzyme structure showed the active site to contain a proximal copper(I) atom; i.e. the dimetallic sub-unit linked to the Fe_4S_4-cluster contained copper(I) and nickel bridged through two cysteinyl thiolate sulfurs. At the time there was only a single example of a thiolate-bridged copper(I)–nickel species [51] but soon after Riordan reported the isolation of discrete dinuclear complexes with nickel in an N_2S_2 coordination environment bridged to copper(I) [52]. The copper(I) atom in these complexes is ligated by two thiolate and two thioether donor atoms in an approximate tetrahedral array (Fig. 13) with one of the four copper–sulfur bond lengths elongated; a similar asymmetry is observed in the A_{Cu}-cluster.

Later protein structures and biochemical studies have led to the consensus that the enzymatically active A-cluster has a nickel–nickel dimetallic sub-site. Rauchfuss reported a structural analogue of this sub-site prepared from the reaction of a nickel diamidodithiolate $[Ni(ema)]^{2-}$, where H_4ema is *N*,*N*′-ethylenebis(2-mercaptoacetamide), with bis(1,5-cyclooctadiene)nickel(0), followed by mild carbonylation [53]. The dinickel complex has a symmetric Ni(0)–Ni(II) structure with the nickel dicarbonyl ligated by the Ni–N_2S_2 chelate ligand (Fig. 14). We have also used $[Ni(ema)]^{2-}$ to prepare the Ni(II)–Ni(II) complexes

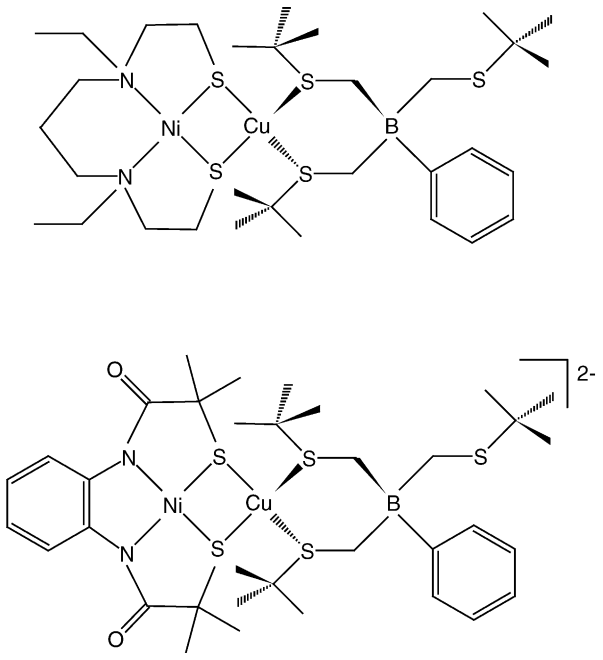

Fig. 13. Copper–nickel dimetallic complexes of relevance to the A_{Cu}-cluster of ACS.

$[Ni(ema)(\mu\text{-}S,S')Ni(dppp)]$ and $[Ni(ema)(\mu\text{-}S,S')Ni(dppe)]$ [54]. The crystal structure (Fig. 15) of the former shows both nickel(II) atoms to be square planar and the two planes are hinged at the shared sulfurs as is also observed in the A_{Ni}-cluster. The phopshine ligands, which are π-acceptors, can be thought of as mimics of bound CO. A related complex, which has diaminodithiolate ligation to one of the nickel atoms, has also been reported [55] and has a similar structure (Fig. 16). Most recently, Riordan has used a tripeptide, Cys-Gly-Cys, as a ligand to nickel to accurately mimic the distal nickel coordination environment [56]. The square planar metallopeptide $[Ni(CGC)]^{2-}$ then can be reacted with $[NiCl_2(diphos)]$ to give a dinickel(II) complex with the closest yet structural analogy to the sub-site of A_{Ni}-cluster (Fig. 17). The Ni(II)–Ni(II) state of this complex does not react with CO but reduced forms do bind CO as shown by cyclic voltammetry.

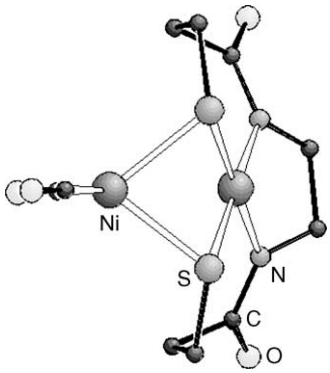

Fig. 14. Crystal structure of the anion $[Ni(ema)(\mu\text{-}S,S')Ni(CO)_2]^{2-}$ [53].

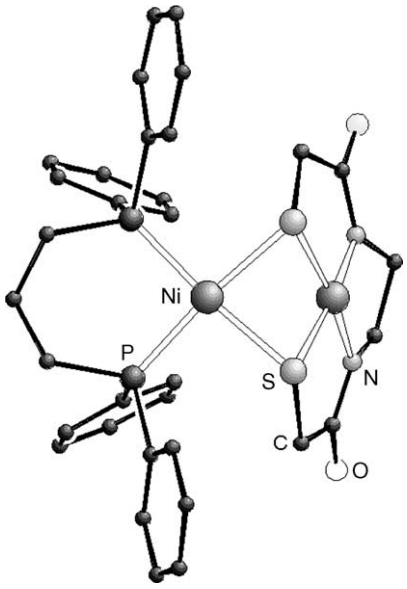

Fig. 15. Crystal structure of the molecule [Ni(ema)(μ-*S*,*S*′)Ni(dppp)] [54].

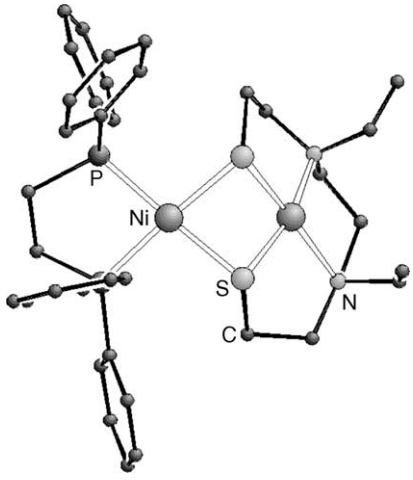

Fig. 16. Crystal structure of the cation $[Ni(dddt)(\mu\text{-}S,S')Ni(dppe)]^{2+}$, where dddt is *N*,*N*′-diethyl-3,7-diazanonane-1,9-dithiolato(2−) [55].

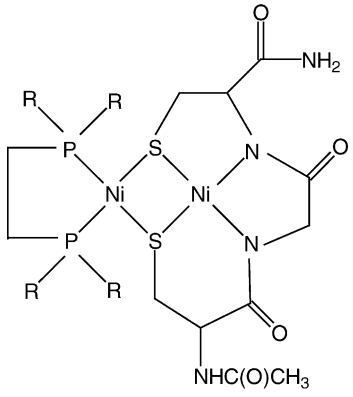

Fig. 17. Schematic representation of [Ni(CGC)(μ-*S*,*S*′)Ni(diphos)], where R is Ph or Et.

The lability of the proximal metal in the A-cluster of ACS has been alluded to above, in addition it has been proposed that the Ni–N_2S_2 distal fragment at the ACS active site is modified after assembly by the capture of copper, zinc or nickel ions to provide the proximal metal [9,10]. Darensbourg has established a chemical precedent for such a process [57]. She has also established a qualitative ranking of $Zn^{2+} < Ni^{2+} < Cu^{+}$ for the metal ion affinity of a model Ni–N_2S_2 complex and demonstrated that both zinc and nickel are labile when bound to this complex. These observations help to explain the observed heterogeneity and variable metal content of the A-cluster.

4.3. Chemical systems of relevance to the mechanism of ACS

The mechanism of ACS action is proposed to involve: CO binding to nickel, methyl transfer to nickel, CO insertion into the nickel-methyl bond (or methyl migration to CO) to give a nickel-acetyl, reaction with CoA to give acetyl-CoA. Each of these steps can be modelled chemically, although so far most examples are at monometallic nickel sites and were described before the complexity of the A-cluster was known.

4.3.1. Nickel-carbonyl complexes

The first step in the proposed mechanisms of ACS action (Schemes 2 and 3) is the formation of a nickel-carbonyl. Nickel-carbonyl complexes have been described above in the context of CODH. Other systems that have some relevance to ACS are described here. Reaction of $[Ni(terpy)Cl_2]$, where terpy is 2,2′,2″-terpyridine, with the bulky thiolate 2,4,6-$(^{i}Pr)_3C_6H_2S^{-}$ (SR) gives pentacoordinated $[Ni(terpy)(SR)_2]$, that can be reduced by dithionite to the nickel(I) complex $[Ni(terpy)(SR)_2]^{-}$, this readily reacts with CO to give $[Ni(terpy)(SR)_2(CO)]$. Spectroscopic evidence is consistent with this complex being octahedral nickel(I) with the three terpy nitrogens and the CO in the equatorial plane with the bulky thiolates *trans* to each other. On oxidation, the coordinated CO dissociates from the complex and will not bind to the oxidised species [58–60]. More recently, a four coordinate nickel(I)-carbonyl, where the other ligands to nickel are thioether sulfurs, $[\{PhTt^{tBu}\}Ni(CO)]$ where $PhTt^{tBu}$ is phenyltris{(*tert*-butylthiol)methyl}borate has been described. Spectroscopy together with semiempirical calculations reveal extensive Ni^{+} to CO π back-bonding interactions [61]. The low C–O stretching frequency observed for this complex at $\nu_{CO} = 1995\ cm^{-1}$ is similar to that observed for ACS-CO [62,63].

4.3.2. Methyl transfer

During enzymatic turnover a methyl group (CH_3^{+}) is transferred to the A-cluster of ACS from the cobalt-methyl moiety of methylated-corrinoid-iron-sulfur protein; the intimate mechanism of this process is still to be elucidated, as is assignment of the nickel redox state [22,23,64]. There are no chemical examples of methyl transfer from cobalt-methyl

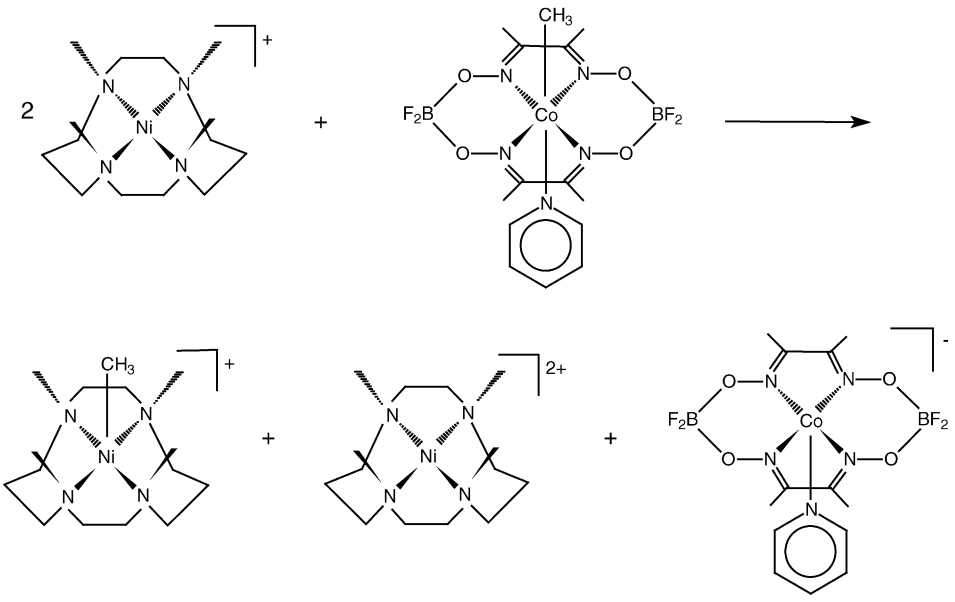

Scheme 5.

to nickel(0) but there is one example for methyl transfer from a CH_3–Co(III) complex to nickel(I) [65,66]. Addition of [(methyl)Co{(difluoroboryl)dimethylglyoximato}$_2$(pyridine)] to two equivalents of [Ni(tmc)OTf], where tmc is 1,4,8,11-tetramethyl-1,4,8,11-tetraazacyclotetradecane and OTf is triflate, gives the products shown in Scheme 5 which include a methyl-nickel(II) complex. The coordination environment about nickel is all nitrogen, unlike the sulfur coordination of the proximal nickel in the A-cluster. The mechanism of reaction (involving nickel(I) reduction of the organocobalt derivative followed by cobalt-methyl bond homolysis) is evidently different to that occurring in ACS, which may be considered more akin to the abstraction of CH_3^+ from CH_3I with elimination of iodide, an example of this reaction facilitated by a nickel(0) complex is given later.

4.3.3. CO insertion reactions, acetyl and thioester formation

The nickel complex [Ni(terpy)$(SR)_2$] described above, on reduction with methyl lithium in solution at low temperature generates the nickel-methyl radical complex formulated as [Ni(terpy)$(SR)_2(CH_3^-)]^{2-}$ but attempts to insert CO into the nickel-methyl bond of this complex were unsuccessful [60]. An example of a monometallic nickel(II)-methyl complex, in an otherwise all-sulfur coordination environment, is provided by $[Ni(CH_3)(MeS_2)_2]^-$, where MeS_2^- is *o*-(methylthio)thiophenolate(1−) (Fig. 18) [67]. In this complex one of the thioether sulfurs is detached from the nickel resulting in a planar {NiS_3C} core. This complex reacts immediately with CO and infra-red spectroscopy provides evidence for the formation of a nickel-acetyl intermediate but the final products remain unidentified.

Several functional models that mimic the CO insertion step with subsequent formation of thioester have been described. [Ni{$N(CH_2CH_2SR)_3$}Cl], where R is ^{i}Pr or ^{t}Bu, can be methylated with methylmagnesium chloride to give $[Ni(N(CH_2CH_2SR)_3)(CH_3)]^+$ (Fig. 19). Carbon monoxide inserts into the nickel-methyl bond of this complex, in solution at low temperature, yielding the acetylated product that was isolated and crystallographically characterised. Reaction of the acetylated complex with a thiol slowly liberates a thioester and releases nickel metal and the protonated free ligand [68]. Sellmann has described a reaction cycle, utilising [Ni($S_4C_3Me_2$)], where $S_4C_3Me_2^{2-}$ is 1,3-bis(2-mercaptophenylthio)-2,2-dimethylpropane(2−) (Fig. 20) for which the net reaction again is the nickel-mediated forma-

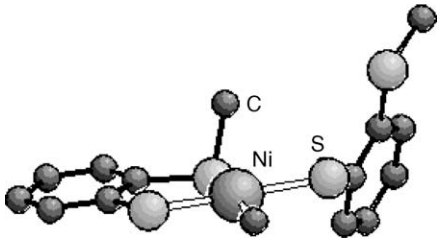

Fig. 18. Crystal structure of the anion $[Ni(CH_3)(MeS_2)_2]^-$, where MeS_2^- is *o*-(methylthio)thiophenolate(1−) [67].

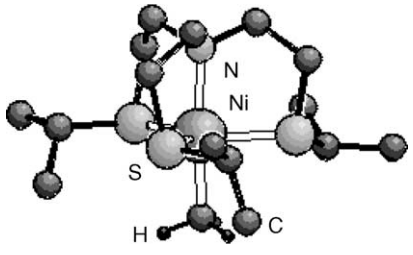

Fig. 19. Crystal structure of the cation $[Ni(N(CH_2CH_2S^iPr)_3)(CH_3)]^+$ [68].

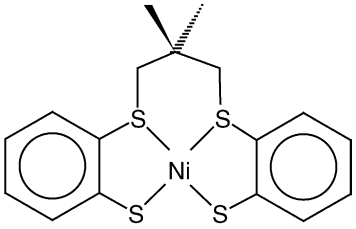

Fig. 20. Schematic representation of [Ni($S_4C_3Me_2$)], where $S_4C_3Me_2^{2-}$ is 1,3-bis(2-mercaptophenylthio)-2,2-dimethylpropane(2−).

tion of thioester from alkyl, CO and thiol groups [69]. Comparable nickel-mediated transformations have been demonstrated also for systems with less physiological-type ligation such as (2,2′-bipyridyl)dimethylnickel(II), Scheme 6; thioester is obtained in yields of 96–100% in situ [70]. In addition, others have also demonstrated CO insertion into nickel-methyl bonds to form nickel-acetyls. For example, Brookhart in the context of ethylene/CO copolymerisation, has discussed four- and five-coordinate CO insertion mechanisms, Scheme 7 [71,72] and Darensbourg has described the formation of Ni(II)-methyl and -acetyl derivatives from the thioether complex $[Ni(Ph_2PCH_2CH_2SEt)_2]^{2+}$ via a nickel(0) species generated in solution, Scheme 8 [73].

These nickel(II) mediated methyl/acetyl transformations with CO, and thioester formation, are processes pertinent to the mechanism of ACS. However, all are at monometallic nickel centres. In our laboratory we have synthesised the first example of a methylated-nickel in a heterodimetallic assembly [74]. Reaction of the iron-nitrosyl chelate, $[Fe(NS_3)(NO)]^-$, with $[NiCl(CH_3)(dppe)]$ gives the methylated-nickel dinuclear complex $[\{Fe(NS_3)(NO)\text{-}S\}Ni(CH_3)(dppe)]$ in which the iron moiety is linked to nickel through a single bridging thiolate (Fig. 21). This complex

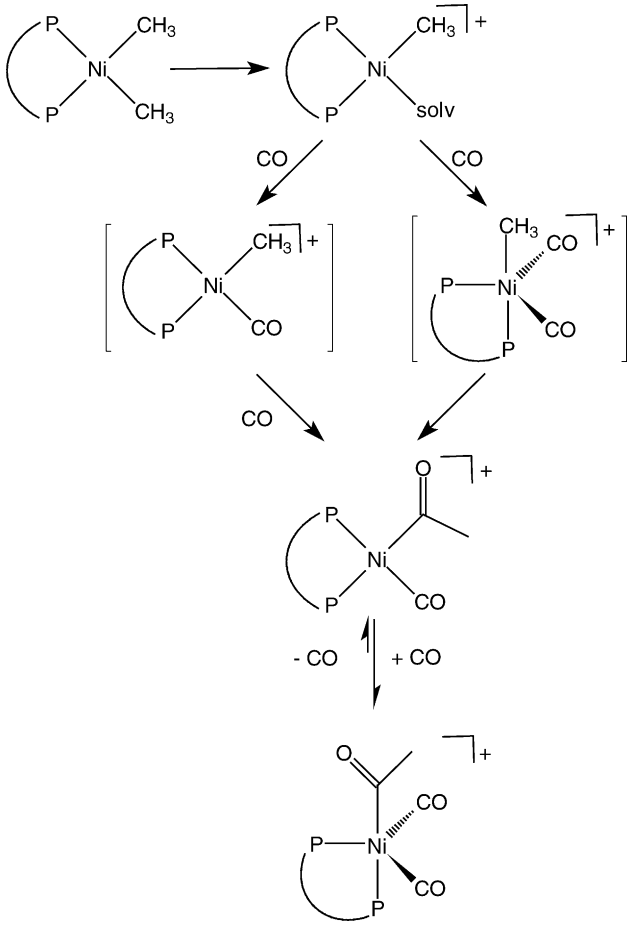

Scheme 7.

can be considered as a first generation analogue of the postulated nickel-methyl intermediate of the ACS mechanism, however, due to its low solubility, insertion of CO into the nickel-methyl bond has not been realised.

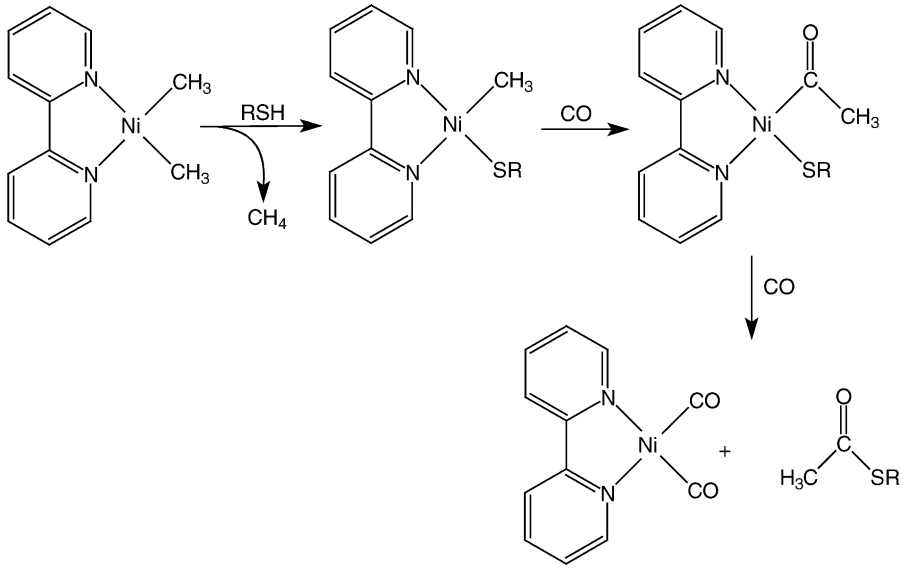

Scheme 6.

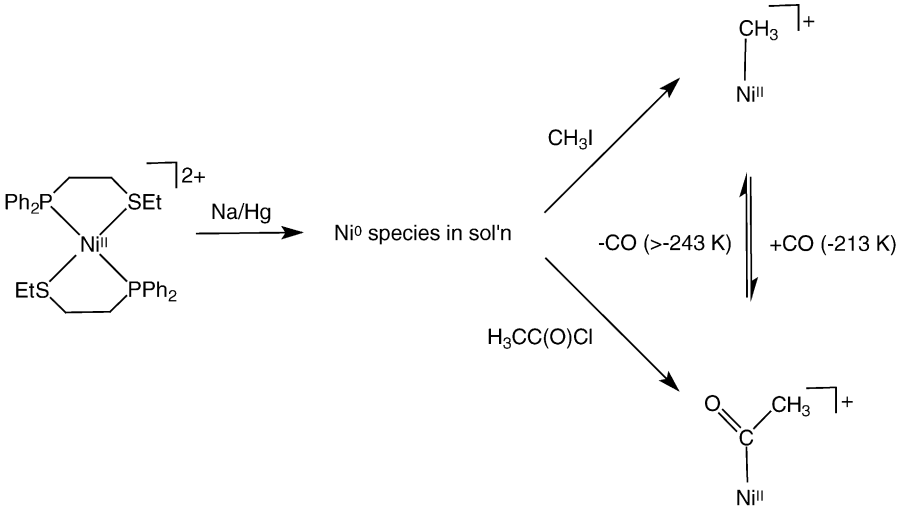

Scheme 8.

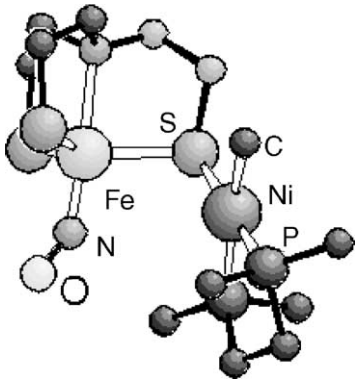

Fig. 21. Crystal structure of [{Fe(NS_3)(NO)-S}Ni(CH_3)(dppe)]. The phenyl groups and all hydrogen atoms have been omitted for clarity [74].

5. Conclusions

Before publication of the CODH and ACS protein crystal structures an extensive chemistry of mononuclear nickel complexes had been developed in the context of the proposed enzyme active site structures and mechanisms of action. When the protein crystal structures were finally determined, the active site structures were unique, different to those predicted, and unprecedented in biology and chemistry. Bioinorganic/coordination chemists have responded to the challenge of designing routes to synthetic structural and functional analogues of these assemblies. Their efforts have been reviewed above. It is anticipated that continued research in this area will not only lead to a better understanding of the enzymes' mechanism but will also generate new catalysts, based on the relatively cheap metals iron and nickel, for CO/CO_2 interconversion, CO_2-fixation and chemical feedstock synthesis.

Acknowledgements

The Biotechnology and Biological Sciences Research Council are thanked for funding and the John Innes Foundation for studentships. Elaine Barclay, Sam Duff, Steven Longhurst and Matt Smith are present and past members of my group who have made valued contributions to the chemistry relating to hydrogenase and CODH/ACS; their efforts are much appreciated. Siân Davies is thanked for X-ray crystallography and assistance in preparing some of the figures in this review.

References

[1] S.W. Ragsdale, M. Kumar, Chem. Rev. 96 (1996) 2515.
[2] J.C. Fontecilla-Camps, S.W. Ragsdale, Adv. Inorg. Chem. 47 (1999) 283.
[3] P.M. Vignais, B. Billoud, J. Meyer, FEMS Micro. Revs. (2001) 455.
[4] V. Svetlitchnyi, C. Peschel, G. Acker, O. Meyer, J. Bacteriol. 183 (2001) 5134.
[5] S.B. Mulrooney, R.P. Hausinger, FEMS Micro. Revs. (2003) 239.
[6] C. Huber, G. Wächtershäuser, Science 276 (1997) 245.
[7] H. Dobbek, V. Svetlitchnyi, L. Gremer, R. Huber, O. Meyer, Science 293 (2001) 1281.
[8] C.L. Drennan, J. Heo, M.D. Sintchak, E. Schreiter, P. Ludden, PNAS 98 (2001) 11973.
[9] C. Darnault, A. Volbeda, E.J. Kim, P. Legrand, X. Vernède, P.A. Lindahl, J.C. Fontecilla-Camps, Nat. Struct. Biol. 10 (2003) 271.
[10] T.I. Doukov, T.M. Iverson, J. Seravalli, S.W. Ragsdale, C.L. Drennan, Science 298 (2002) 567.
[11] P.A. Lindahl, Biochemistry 41 (2002) 2097.
[12] C.L. Drennan, J.W. Peters, Curr. Opin. Struct. Biol. 13 (2003) 220.
[13] W. Gu, J. Seravalli, S.W. Ragsdale, S.P. Cramer, Biochemistry 43 (2004) 9029.
[14] H. Dobbek, V. Svetlitchnyi, J. Liss, O. Meyer, J. Am. Chem. Soc. 126 (2004) 5382.
[15] J. Feng, P.A. Lindahl, J. Am. Chem. Soc. 126 (2004) 9094.
[16] V. Svetlitchnyi, H. Dobbek, W. Meyer-Klaucke, T. Meins, B. Thiele, P. Römer, R. Huber, O. Meyer, PNAS 101 (2004) 446.

[17] W.-W. Gu, S. Gencic, S.P. Cramer, D.A. Grahame, J. Am. Chem. Soc. 125 (2003) 15343;
T. Funk, W.-W. Gu, S. Friedrich, H. Wang, S. Gencic, D.A. Grahame, S.P. Cramer, J. Am. Chem. Soc. 126 (2004) 88.
[18] S. Gencic, D.A. Grahame, J. Biol. Chem. 278 (2003) 6101.
[19] M.R. Bramlett, X. Tan, P.A. Lindahl, J. Am. Chem. Soc. 125 (2003) 9316;
X. Tan, M.R. Bramlett, P.A. Lindahl, J. Am. Chem. Soc. 126 (2004) 5954.
[20] J. Seravalli, Y. Xiao, W. Gu, S.P. Cramer, W.E. Antholine, V. Krymov, G.J. Gerfen, S.W. Ragsdale, Biochemistry 43 (2004) 3944.
[21] C.L. Drennan, T.I. Doukov, S.W. Ragsdale, J. Biol. Inorg. Chem. 9 (2004) 511.
[22] P.A. Lindahl, J. Biol. Inorg. Chem. 9 (2004) 516.
[23] A. Volbeda, J.C. Fontecilla-Camps, J. Biol. Inorg. Chem. 9 (2004) 525.
[24] J. Seravalli, M. Kumar, S.W. Ragsdale, Biochemistry 41 (2002) 1807.
[25] C.G. Riordan, J. Biol. Inorg. Chem. 9 (2004) 542.
[26] F. Osterloh, W. Saak, S. Pohl, J. Am. Chem. Soc. 119 (1997) 5648.
[27] F. Osterloh, W. Saak, D. Haase, S. Pohl, Chem. Commun. (1996) 777.
[28] C.R. Staples, J. Heo, N.J. Spangler, R.L. Kerby, G.P. Roberts, P.W. Ludden, J. Am. Chem. Soc. 121 (1999) 11034;
J. Heo, C.R. Staples, C.M. Halbleib, P.W. Ludden, Biochemistry 39 (2000) 7956.
[29] S.C. Davies, D.L. Hughes, R.L. Richards, J.R. Sanders, J. Chem. Soc., Dalton Trans. (2000) 719;
S.C. Davies, M.C. Durrant, D.L. Hughes, R.L. Richards, J.R. Sanders, J. Chem. Soc., Dalton Trans. (2000) 4694.
[30] M.C. Smith, S. Longhurst, J.E. Barclay, S.P. Cramer, S.C. Davies, D.L. Hughes, W.-W. Gu, D.J. Evans, J. Chem. Soc., Dalton Trans. (2001) 1387.
[31] M.C. Smith, J.E. Barclay, S.P. Cramer, S.C. Davies, W.-W. Gu, D.L. Hughes, S. Longhurst, D.J. Evans, J. Chem. Soc., Dalton Trans. (2002) 2641.
[32] F. Barrière, D.J. Evans, D.L. Hughes, S.K. Ibrahim, J. Talarmin, C.J. Pickett, J. Chem. Soc., Dalton Trans. (1999) 957.
[33] C. Chen, T. Wen, W. Li, H. Zhu, Y. Chen, Q. Liu, J. Lu, Inorg. Chem. 38 (1999) 2375.
[34] S. Ciurli, P.K. Ross, M.J. Scott, S.-B. Yu, R.H. Holm, J. Am. Chem. Soc. 114 (1992) 5415.
[35] J. Zhou, M.J. Scott, Z. Hu, G. Peng, E. Münck, R.H. Holm, J. Am. Chem. Soc. 114 (1992) 10843.
[36] J. Zhou, J.W. Raebiger, C.A. Crawford, R.H. Holm, J. Am. Chem. Soc. 119 (1997) 6242.
[37] R. Panda, Y. Zhang, C.C. McLauchlan, P.V. Rao, T. de Oliveira, E. Münck, R.H. Holm, J. Am. Chem. Soc. 126 (2004) 6448.
[38] T. Yamamura, S. Sakurai, H. Arai, H. Miyamae, Chem. Commun. (1993) 1656.
[39] D.H. Nguyen, H.-F. Hsu, M. Millar, S.A. Koch, C. Achim, E.L. Bominaar, E. Münck, J. Am. Chem. Soc. 118 (1996) 8963.
[40] Z. Lu, R.H. Crabtree, J. Am. Chem. Soc. 117 (1995) 3994.
[41] D.J. Evans, C.J. Pickett, Chem. Soc. Rev. 32 (2003) 268.
[42] C.-H. Lai, J.H. Reibenspies, M.Y. Darensbourg, Angew. Chem., Int. Ed. Engl. 35 (1996) 2390.
[43] F. Osterloh, W. Saak, D. Hasse, S. Pohl, Chem. Commun. (1997) 979.
[44] S.C. Davies, D.J. Evans, D.L. Hughes, S. Longhurst, J.R. Sanders, Chem. Commun. (1999) 1935.
[45] S.E. Duff, S.C. Davies, D.J. Evans, Unpublished results.
[46] A.C. Marr, D.J.E. Spencer, M. Schröder, Coord. Chem. Rev. 219–221 (2001) 1055.
[47] D. Sellmann, F. Geipel, F. Lauderbach, F.W. Heinemann, Angew. Chem. Int. Ed. 41 (2002) 632.
[48] C.E. Laplaza, R.H. Holm, J. Am. Chem. Soc. 123 (2001) 10255.
[49] C.E. Laplaza, R.H. Holm, J. Biol. Inorg. Chem. 7 (2002) 451.
[50] K.B. Musgrave, C.E. Laplaza, R.H. Holm, B. Hedman, K.O. Hodgson, J. Am. Chem. Soc. 124 (2002) 3083.
[51] D.C. Jicha, D.H. Busch, Inorg. Chem. 1 (1962) 878.
[52] R. Krishnan, J.K. Voo, C.G. Riordan, L. Zahkarov, A.L. Rheingold, J. Am. Chem. Soc. 125 (2003) 4422.
[53] R.C. Linck, C.W. Spahn, T.B. Rauchfuss, S.R. Wilson, J. Am. Chem. Soc. 125 (2003) 8700.
[54] J.E. Barclay, S.C. Davies, S.E. Duff, D.J. Evans, 15th Summer School on Coordination Chemistry, Perspectives in Coordination Chemistry, Szklarska Poręba, Poland, June 6–12, 2004.
[55] Q. Wang, A.J. Blake, E.S. Davies, E.J.L. McInnes, C. Wilson, M. Schröder, Chem. Commun. (2003) 3012.
[56] R. Krishnan, C.G. Riordan, J. Am. Chem. Soc. 126 (2004) 4484.
[57] M.L. Golden, M.V. Rampersad, J.H. Reibenspies, M.C. Darensbourg, Chem. Commun. (2003) 1824.
[58] N. Baidya, M. Olmstead, P.K. Mascharak, Inorg. Chem. 30 (1991) 929.
[59] N. Baidya, M.M. Olmstead, P.K. Mascharak, J. Am. Chem. Soc. 114 (1992) 9666.
[60] N. Baidya, M.M. Olmstead, J.P. Whitehead, C. Bagyinka, M.J. Maroney, P.K. Mascharak, Inorg. Chem. 31 (1992) 3612.
[61] J.L. Craft, B.S. Mandimutsira, K. Fujita, C.G. Riordan, T.C. Brunold, Inorg. Chem. 42 (2003) 859.
[62] M. Kumar, S.W. Ragsdale, J. Am. Chem. Soc. 114 (1992) 8713.
[63] J. Chen, S. Huang, J. Seravalli, H. Gutzman Jr., D.J. Swartz, S.W. Ragsdale, K.A. Bagley, Biochemistry 42 (2003) 14822.
[64] T. Brunold, J. Biol. Inorg. Chem. 9 (2004) 533.
[65] M.S. Ram, C.G. Riordan, J. Am. Chem. Soc. 117 (1995) 2365.
[66] S.W. Ragsdale, C.G. Riordan, J. Biol. Inorg. Chem. 1 (1996) 489.
[67] D. Sellmann, H. Schillinger, F. Knoch, M. Moll, Inorg. Chim. Acta 198–200 (1992) 351.
[68] P. Stavropoulos, M.C. Muetterties, M. Carrié, R.H. Holm, J. Am. Chem. Soc. 113 (1991) 8485.
[69] D. Sellmann, D. Häussinger, F. Knoch, M. Moll, J. Am. Chem. Soc. 118 (1996) 5368.
[70] G.C. Tucci, R.H. Holm, J. Am. Chem. Soc. 117 (1995) 6489.
[71] C.S. Shultz, J.M. DeSimone, M. Brookhart, Organometallics 20 (2001) 16.
[72] C.S. Shultz, J.M. DeSimone, M. Brookhart, J. Am. Chem. Soc. 123 (2001) 9172.
[73] Y.-M. Hsiao, S.S. Chojnacki, P. Hinton, J.H. Reibenspies, M.Y. Darensbourg, Organometallics 12 (1993) 870.
[74] M.C. Smith, J.E. Barclay, S.C. Davies, D.L. Hughes, D.J. Evans, Dalton Trans. (2003) 4147.